

Article

# A Load Flow Analysis for AC/DC Hybrid Distribution Network Incorporated with Distributed Energy Resources for Different Grid Scenarios

Muhammad Omer Khan, Saeed Zaman Jamali, Chul-Ho Noh, Gi-Hyeon Gwon and Chul-Hwan Kim \*

College of Information and Communication Engineering, Sungkyunkwan University, Suwon 440-746, Korea; omerkhan@skku.edu (M.O.K.); saeedzaman@skku.edu (S.Z.J.); chcoo87@skku.edu (C.-H.N.); elysium03@skku.edu (G.-H.G.)

\* Correspondence: chkim@skku.edu; Tel.: +81-31-290-7124

Received: 28 December 2017; Accepted: 30 January 2018; Published: 4 February 2018

**Abstract:** With the recent developments in power electronics technologies, increased deployment of distributed energy resources (DER) with DC output type at distribution voltage levels and significant increase in the number of sensitive AC and DC loads integrated in distribution network have enforced the traditional power network in the continuous renovation process. In this paper, the load flow solution of hybrid AC/DC distribution networks with the multi-terminal configuration is studied. The impact of voltage source converter (VSC) losses and AC and DC line losses in the presence of DER in the distribution system are assessed. The motivation of this analysis is to consider an increase in the number of converter stations which might result in non-negligible converter losses and the presence of various DER within the network imposing different network scenarios. The proposed schemes are simulated on two modified IEEE 33 bus hybrid AC/DC distribution network test system equipped with VSC-MTDC and the results are presented. Obtained results show that by considering the network losses and the converter losses with large number of converters within the network could lead to very different load flow solution and power transfer between networks, especially considering the AC or DC bus dominated network.

**Keywords:** load flow analysis; AC/DC hybrid distribution network; distributed energy resources; voltage source converter multi-terminal DC (VSC-MTDC)

## 1. Introduction

The main challenges of current power systems are to meet the ever growing requirements for higher quality and reliability of electricity in a sustainable, secure and competitive manner in distribution systems [1]. Recent significant advancements in power electronic technologies, renewable based distributed energy resources (DER), flexible AC transmission systems (FACTS), energy storage systems (ESSs), and advanced control strategies based on information and communication technologies (ICTs) have motivated redesigning the power system with integrated AC and DC microgrids [2,3]. In addition, the hybrid AC and DC microgrids should be smart enough to integrate, control and manage the growing rate of deploying DC output type distributed generations (DGs), energy storage systems, and increasing number of DC electronic loads [4–6]. This new concept of hybrid AC/DC distribution network could fully demonstrate the advantages of partially AC and DC networks by facilitating in the decoupling and power exchanges between the networks using bi-directional converters [7–10]. In general, the advantages of hybrid AC/DC distribution network can be summarized as [11]: (1) Reduction in the number of power conversion circuits in the power supply will reduce the power conversion losses; (2) Simplified equipment, reduce

costs and losses by eliminating power electronics equipment used as end-users for power quality improvement, harmonics reduction and power factor correction; (3) No need to track phase, frequency and unsymmetrical current flow problems caused by unbalanced loads in AC grid; and (4) Easy integration of DER and ESS [12–14].

A feasible solution for AC/DC hybrid network emerged from the development in the Voltage Source Converter (VSC) based technology. VSC-based technologies offer significant advantages such as low cost, reduction in the size of the converter, reliable operation with weak AC systems. With the VSC technology, the extension to multi-terminal HVDC (MTDC) are recently involved under intensive research, such as Desertec project [15] and the European Offshore Supergrid [16]. VSC-based technologies offer significant advantages such as low cost, reduction in the size of the converter, reliable operation with weak AC systems. Due to completely different principles of operation of VSC-MTDC networks, different researchers have recently covered various technical issues, such as stability analysis [17], control strategies [18–20], locating of DC fault and protection [21,22], integrating wind farms [23] and dynamic modeling for power system simulation [24].

For steady state modeling of the load flow solution of the hybrid AC/DC network with VSC-MTDC systems, two different approaches have been reported in the literature: sequential [25] and unified [26]. The difference between the approaches is the applied procedure for the integration of AC and DC network equations. A comprehensive multi-terminal VSC-HVDC newton power flow model suitable for different VSC interconnection configurations was presented in [27–29]. In [29], VSCs are treated as compound transformer devices that take into account their inductive and capacitive power design limits along with switching and ohmic losses. In another study, a steady-state VSC-MTDC model includes DC grids with arbitrary topologies considering converter transformer losses [25], unlike [30], where an approximate solution is obtained by neglecting converter losses and losses in the phase reactor. A novel power flow approach for MTDC systems with different network topologies incorporating different DC voltage strategies was presented in [31]. In the case of large deployments of VSC-MTDC networks, the impact of converter stations in the operation and control along with energy conversion process needs to be carefully examined. As in any converter, the energy transformation operation is not 100% efficient due to constraints imposed by the power electronic equipment. Typical values for conversion losses ranges from 1% to 3% of the total power injected or withdrawn through the converter [32]. For large VSC-MTDC networks, the active power losses of the converter could represent a significant portion of all the losses and cannot be neglected [33–35]. Along with converter characteristics, the focus of this paper is to assess the impact of converter losses along with the network losses [36,37] on the load flow solution for the hybrid AC/DC distribution network. In addition, the effects of integration of DGs in hybrid AC/DC distribution networks are complicated and have to be carefully examined [38,39].

In this paper, a mathematical model for VSC is explored for proper modeling of converter losses, which are computed as a polynomial function that depends on the phase current of the converter, taking into account the difference in losses type when the converter acts as a rectifier or an inverter. In addition, in this assessment, the impact of converter losses on the load flow solution along with the losses in AC and DC distribution networks facilitated with DGs connection at appropriate locations is studied in term of effectively reducing the network losses. Two different network scenarios are presented by modifying IEEE 33 bus AC/MTDC distribution networks for the validation of results.

This paper is structured as follow: In Section 2, a mathematical model of VSC-Station is described which includes the reactor, filter, converter losses and also discusses the operating modes. Section 3 defines the generalized AC/DC network load flow algorithm. Section 4 shows the VSC-based proposed topologies and addresses the proposed scenarios with the integration of DER at different location. Finally, the simulation results are compared and discussed in Section 5. The sequential load flow algorithm is implemented in an open source Matlab toolbox, MATPOWER [40].

## 2. VSC Station Model and Operation Modes

This work starts with a description of the VSC station model and its operational modes classification. A VSC station consists of all the elements that connects the AC and DC networks. Based on these operational features, the load flow results of hybrid AC/DC distribution system are discussed.

### 2.1. Types of VSC

VSC-MTDC technology based on Modular Multilevel Converter (MMC) approach [41] has several advantages such as reduced harmonics and reduced transformer  $dv/dt$  stress, and can be foreseen as the technology of the future for VSC-MTDC networks. VSC typically uses insulated-gate bipolar transistors (IGBTs), and the voltage waveform is synthesized by Pulse Width Modulation (PWM) along with phase reactor, DC capacitor and low pass filters essential for blocking the flow of higher order harmonics. PWM is based on two- or three-level VSC topologies enabling a controlled two- or three-level voltage output [42]. Without loss of generality, the approach adopted in this paper for converter modeling does not consider converter type and will be explained further in detail.

### 2.2. VSC-MTDC Power Injection Modeling and Operation

In VSC-MTDC based hybrid AC/DC distribution system, the VSC converter station forms the basic link between AC and DC networks. The phase reactor and filter bus is connected to the AC network through a transformer and the power can flow in both directions. The converter is said to be operating as rectifier when the active power is taken from the AC side and injected into the DC network, otherwise it is operated as an inverter when flow of active power is reversed from the DC side to AC network. The equivalent circuit model for the VSCs is represented in Figure 1 showing different components such as an AC bus, a converter transformer, a phase reactor, an AC filter, a converter block on the AC and DC sides, and a DC bus [25].

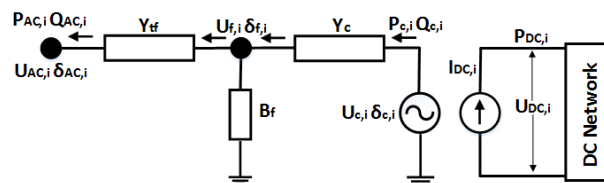


Figure 1. VSC-Station equivalent circuit model.

According to the equivalent circuit model of the VSC represented in Figure 1, the VSC acts as a controllable voltage source represented by  $U_c = U_c \angle \delta_c$ , presented by complex admittance  $Y_c = G_c + jB_c$  behind the phase reactor. The low pass AC filter is represented as a susceptance  $jB_f$ . The converter transformer interfacing filter bus to the AC network is represented by complex admittance  $Y_{tf} = G_{tf} + jB_{tf}$ . The complex grid side voltage outputs at AC and DC buses are represented as  $U_{AC} = U_{AC} \angle \delta_{AC}$  and  $U_{DC}$ , respectively. Along with this, the  $U_f = U_f \angle \delta_f$  and  $U_{tf} = U_{tf} \angle \delta_{tf}$ , respectively, show the filter bus voltage and interface transformer voltage. The power injected to AC network is  $P_{AC}$ ,  $Q_{AC}$  and the power flowing to AC network from the converter side is  $P_c$ ,  $Q_c$  while the DC power is shown by  $P_{DC}$ . The equations for active and reactive power injected into AC network in term of complex voltages are

$$P_{AC} = -U_{AC}^2 G_{tf} + U_{AC} U_{tf} [G_{tf} \cos(\delta_{AC} - \delta_f) + B_f \sin(\delta_{AC} - \delta_f)] \quad (1)$$

$$Q_{AC} = U_{AC}^2 B_{tf} + U_{AC} U_{tf} [G_{tf} \sin(\delta_{AC} - \delta_f) - B_f \cos(\delta_{AC} - \delta_f)] \quad (2)$$

$$P_c = U_c^2 G_c - U_{AC} U_c [G_c \cos(\delta_{AC} - \delta_c) - B_c \sin(\delta_{AC} - \delta_c)] \quad (3)$$

$$Q_c = -U_c^2 B_c + U_{AC} U_c [G_c \sin(\delta_{AC} - \delta_c) + B_c \cos(\delta_{AC} - \delta_c)] \quad (4)$$

Modification in the transformer admittance and/or the filter susceptance can be implemented accordingly in the above equations.

### 2.3. Modeling Converter Losses

Various approaches for the modeling of converter losses are: Modular Multilevel Converter (MMC) approach [43] includes a linear loss model and ABB HVDC Light model approach [44] in which the converters are modeled as generators and no DC line is modeled but this model does not include losses. Thus, these models are of simplified type and there is a need for a more general approach to include converter losses in load flow calculations. A generalized model to represent the losses of the VSC station can take into account the filter losses, phase reactor losses and the drop in transformer impedance [45]. Thus, in this study, a formula used to represent converter losses depends on the magnitude of the converter current  $I_c$  [46] in a quadratic form. The converter current magnitude depends upon the active and reactive power flowing through the converter as shown in Equation (5).

$$I_c = \frac{\sqrt{P_c^2 + Q_c^2}}{\sqrt{3}U_c} \quad (5)$$

whereas the total converter losses  $P_{loss}$  represented by Equation (6) is a combination of constant, linear and variable components [24]. Constant losses are circuit losses associated with the off-state of the device, while linear losses are associated with the switching losses related to current state, the variable losses are associated with generated heat loss and reverse recovery loss.

$$P_{loss} = A + B \cdot I_c + C \cdot I_c^2 \quad (6)$$

where  $A$ ,  $B$ , and  $C$  represents the per unit loss coefficients and depend upon the test data of the converter losses of VSC.

### 2.4. Converter Control Modes

Voltage source converter facilitates multiple control modes by independently controlling the active and reactive power with respect to the AC system. We can represent these control modes with respect to the active power and reactive power in the following different ways [47]:

Mode (1) Constant  $P_{AC}$ -control mode: The converter controls its constant active power injection  $P_{AC}$  into the AC grid.

Mode (2) Constant  $U_{DC}$ -control mode: The converter controls its constant DC bus voltage  $U_{DC}$  irrespective of the converter's active power injection  $P_{AC}$ .

Mode (3) Constant  $Q_{AC}$ -control mode: The converter controls its constant reactive power injection  $Q_{AC}$  into the AC grid.

Mode (4) Constant  $U_{AC}$ -control mode: The converter controls its constant AC bus voltage  $U_{AC}$  by adjusting the reactive power injection  $Q_{AC}$ .

## 3. Sequential AC/DC Load Flow Algorithm

In this section, the sequential AC/DC load flow algorithm is implemented on AC/DC hybrid distribution system incorporated with VSC. Figure 2 shows the flow chart of the sequential load flow algorithm. This algorithm can also facilitate systems having multiple AC and DC interconnected networks and also accommodate those DC buses with no AC grid connection.

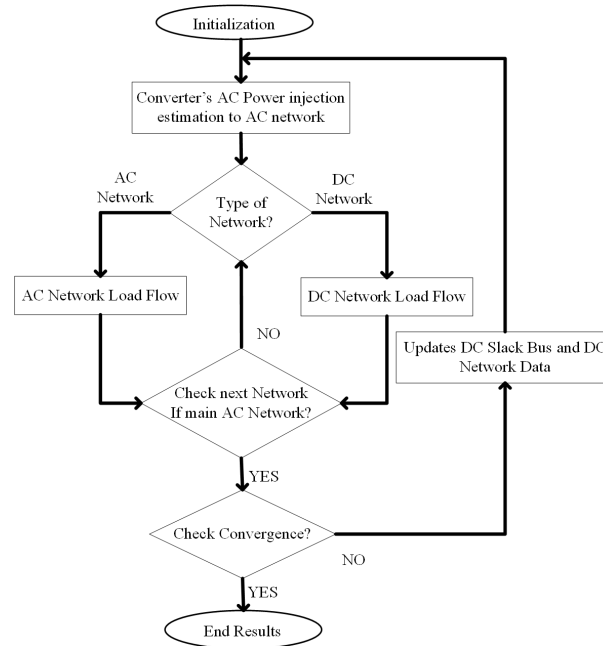


Figure 2. Flow chart of the sequential AC/DC load flow algorithm.

- Step 1: Data input and per unit conversion: The algorithm starts with having all converter data and the AC and DC networks data converted to per unit (p.u) on the same base value.
- Step 2: Determine the converter’s AC power injection for AC networks: At the start of the algorithm, the DC network and converters are assumed to be lossless. In this step, to initiate the iteration, the initial value for converter active power injection to the AC network is estimated by putting it equal to negative of the DC power reference using Equation (7).

The active power injected by the converter is estimated by

$$P_{AC,n} = - \sum_{j=1}^{n-1} P_{AC,j} \tag{7}$$

The vector representation for active power injection into the AC network can be written as

$$P_{AC} = \begin{bmatrix} \underbrace{P_{AC,n}}_{\text{Slack}} \underbrace{P_{AC2}, P_{AC3} \dots P_{AC,n-1}}_{\text{P-control}} \dots \underbrace{0 \dots 0}_{\text{unconnected}} \end{bmatrix}^T \tag{8}$$

where  $n$  represents the total number of converter connected in MTDC network. The  $n$ th converter is considered to be connected with the DC slack bus and the subsequent  $n - 1$  converters buses are considered to be under the constant active power control. The remaining buses are assumed to be not connected to the AC network.

- Step 3: Determine the characteristic of the network: If the network is AC go to Step 4, else if the network is DC go to Step 6.
- Step 4: AC network load flow: During AC network load flow, all converter and DC networks data are considered to be constant. The active and reactive power equations for load flow of AC network can be written as

$$P_i(U, \delta) = U_i \sum_{j=1}^m U_j [G_{ij} \cos(\delta_i - \delta_j) + B_{ij} \sin(\delta_i - \delta_j)] \tag{9}$$

$$Q_i(U, \delta) = U_i \sum_{j=1}^m U_j [G_{ij} \sin(\delta_i - \delta_j) - B_{ij} \cos(\delta_i - \delta_j)] \quad (10)$$

where  $m$  is the total number of AC network buses. The converter power injection  $P_{AC,i}$  and  $Q_{AC,i}$  are included in the power mismatch vectors  $\Delta P$  and  $\Delta Q$  as negative loads. The mismatch vectors can be represented as

$$\Delta P_i = P_i^{Gen} - P_i^{Load} - P_i(U, \delta) + P_{AC,i} \quad (11)$$

$$\Delta Q_i = Q_i^{Gen} - Q_i^{Load} - Q_i(U, \delta) - Q_{AC,i} \quad (12)$$

where  $P_i^{Gen}$  and  $Q_i^{Gen}$  represent the active and reactive power generators connected to AC network buses;  $P_i^{Load}$  and  $Q_i^{Load}$  represent the load connected at AC network buses;  $P_{AC,i}$  and  $Q_{AC,i}$  represent the active and reactive power injection by VSC converters; and  $P_i(U, \delta)$  and  $Q_i(U, \delta)$  represent the active and reactive power of AC network buses calculated by the AC load flow.

Now, the non-linear set of load flow equations are solved by using Newton–Raphson (N-R) load flow algorithm to determine the voltages and phase angles for all the AC buses using Equation (13)

$$\begin{bmatrix} \Delta \delta \\ \frac{\Delta U}{U} \end{bmatrix} = -[J]^{-1} \begin{bmatrix} \Delta P \\ \Delta Q \end{bmatrix} \quad (13)$$

Step 5: Calculation of converter's power and losses: After the AC network load flow calculation, the AC buses voltages  $U_{AC,i}$ , all converters active  $P_{AC,i}$  and reactive  $Q_{AC,i}$  power injection to AC network side and losses  $P_{loss}$  are calculated using Equations (1)–(4) and (6).

Step 6: DC Network load flow: First the injected power  $P_{DC,i}$  to the DC network for the converter connected DC buses can be calculated as

$$P_{DC,i} = -P_{c,i} - P_{loss,i} \forall i \leq n \quad (14)$$

Here,  $P_{c,i}$  represents the active part of the complex power injection at the converter side.

The DC network load flow is similar to the conventional AC network load flow, while not considering the reactive power and line reactance, as it does not play any role in DC network. The conductance matrix  $G_{DC}$  for the DC network can be represented as

$$G_{DC} = \begin{bmatrix} G_{11} & G_{12} & \cdots & G_{1p} \\ G_{21} & G_{22} & \cdots & G_{2p} \\ \vdots & \vdots & \ddots & \vdots \\ G_{p1} & G_{p1} & \cdots & G_{pp} \end{bmatrix} \quad (15)$$

$$G_{DCii} = \sum_{j=1, j \neq i}^p g_{ij}, G_{DCij} = -g_{ij}, i \neq j \quad (16)$$

Here, “ $p$ ” represents the total number of DC buses. The currents injection for DC network can be written as

$$I_{DC} = G_{DC} U_{DC} \quad (17)$$

$$I_{DC,i} = \sum_{j=1, j \neq i}^p G_{DCij} (U_{DC,i} - U_{DC,j}) \quad (18)$$

Here,  $U_{DC} = [U_{DC1}, U_{DC2} \dots U_{DCn}]^T$  represents the DC voltage vector and  $I_{DC} = [I_{DC1}, I_{DC2} \dots I_{DCn}]^T$  represents the DC current vector.

The active power injection  $P_{DC,i}$  for DC network can be calculated as

$$P_{DC,i} = T_o U_{DC,i} \sum_{j=1, j \neq i}^p G_{DCij} (U_{DC,i} - U_{DC,j}) \quad (19)$$

where  $T_o$  defines the configuration of the DC network,  $T_o = 1$  is used for mono-polar configuration and  $T_o = 2$  for bipolar configuration.

The DC bus voltages are calculated using N-R algorithm as

$$\left( U_{DC} \frac{\partial P_{DC}}{\partial U_{DC}} \right) \cdot \frac{\Delta U_{DC}}{U_{DC}} = \Delta P_{DC} \quad (20)$$

Step 7: Determine the network characteristics: If the network is grid connected AC network, go to Step 8, else, if the network is not the grid connected AC network, go to Step 4, else, if the network is DC, go to Step 5.

Step 8: After calculating all the unknowns in DC and AC networks, an additional iteration is needed to calculate the active power injected into the AC network at the converter side  $P_{c,n}$  which depend on the DC slack bus power  $P_{DC,n}$  and the converter losses  $P_{loss,n}$ , as shown in Equation (21)

$$P_{c,n} = -P_{DC,n} - P_{loss,n} \forall i \leq n \quad (21)$$

During this iteration, the AC network side voltage  $U_{AC}$  and reactive power injection into AC network  $Q_{AC}$  are assumed to be constant.

Step 9: Convergence criteria: The convergence criteria in sequential AC/DC algorithm is set by the difference of the active power injected into the AC network at the converter side, as shown in Equation (22)

$$|P_{c,n}^k - P_{c,n}^{k-1}| < \varepsilon \quad (22)$$

where “ $k$ ” and “ $\varepsilon$ ” are referred to as load flow iteration number and the tolerance value for the convergence checking, respectively.

If the result converged, the calculation is complete, else return to Step 2 with updated values of AC and DC networks acquired at current iteration.

#### 4. AC/DC Hybrid Distribution Network Models

The IEEE 33 bus distribution test network [48] was modified for this case study. The two proposed topologies for AC/DC hybrid distribution system consist of AC network and embedded DC network as shown in Figures 3 and 4. This modeling approach of modification of topologies do not impose any restriction in term of configuration and topology for AC and DC networks, and this design can also accommodate the interconnection of different types of DER into the hybrid AC/DC system.

The base power, base AC voltage value, and base DC voltage are 100 MVA, 12.66 kV and 1.5 kV, respectively. The data for voltage and power are shown in per unit (p.u). The resistances and leakage reactance of all the converter transformer were taken as  $0.0015 + j0.1121$  p.u. The filter susceptance was taken as  $j0.045$  p.u and reactor impedance was taken as  $0.0001 + j0.1643$  p.u.

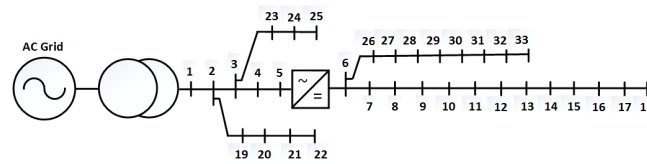


Figure 3. AC/DC Hybrid models—Topology 1.

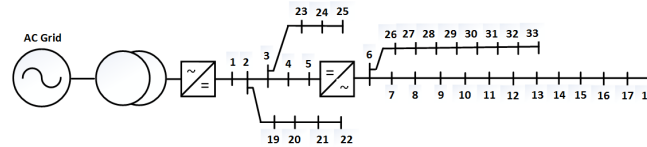


Figure 4. AC/DC Hybrid models—Topology 2.

#### 4.1. AC/DC Hybrid Distribution System—Topology 1

The proposed Topology 1 of AC/DC hybrid distribution test network is shown in Figure 3. In this topology, the VSC converter is added between bus 5 and 6 modifying the topology into AC/DC network. In this DC bus dominated topology, the ratio of AC to DC buses becomes 1:2. In addition, in this topology, the AC bus 1 is selected as the AC slack bus with AC voltage amplitude of 1.05 p.u and phase angle zero. In DC network, the DC bus 6 is selected as the DC slack bus with DC voltage amplitude of 1.05 p.u. Voltage amplitudes and phases of the rest of the AC buses are 1 p.u with angle zero degree and DC buses voltage amplitudes are 1.0 p.u as flat start is considered for this simulations.

#### 4.2. AC/DC Hybrid Distribution System—Topology 2

The proposed Topology 2 of AC/DC hybrid distribution test network is shown in Figure 4. In this topology, VSC converters are added at the start of the network and between bus 5 and 6. This topology is different from topology 1 in such a way that it is AC buses dominated system with a ratio of AC to DC buses to be 2:1. In this topology, the AC bus 6 is the AC slack bus with AC voltage amplitude of 1.05 p.u, the DC bus 1 is selected as the DC slack bus with DC voltage amplitude of 1.05 p.u. The voltage amplitudes and phases of the rest of the AC buses are 1 p.u with angle zero degrees while DC buses voltage amplitudes are 1.0 p.u as flat start is considered for this simulations.

With distributed energy resources (DER) connected at appropriate locations, as given in Tables 1 and 2, the following three scenarios are studied:

Scenario (1): All DER are connected at the AC network side with only AC type output.

Scenario (2): All DER are connected at the DC network side with only DC type output.

Scenario (3): DER are connected in both AC and DC networks depending upon the DER output type. In this study, the DER and loads are modeled as constants without consideration the varying nature of distributed energy sources whose output depend upon many natural factors.

Table 1. Summary of connected Distribution Energy Resources (DER) to Topology 1.

	PV	Wind	Fuel Cells	Gas Turbine
AC Buses Only	21	24	2	4
DC Buses Only	26	7	32	17
Hybrid AC/DC Buses	26	24	32	4
Capacity (MW)	0.5	0.5	0.3	0.3

**Table 2.** Summary of connected Distribution Energy Resources (DER) to Topology 2.

Source	PV	Wind	Fuel Cells	Gas Turbine
AC Buses Only	26	7	32	17
DC Buses Only	21	24	2	4
Hybrid AC/DC Buses	21	7	2	17
Capacity (MW)	0.5	0.5	0.3	0.3

## 5. Load Flow Simulation and Results

The load flow results for the above proposed topologies are presented in this section. A convergence tolerance of  $10^{-4}$  p.u is adopted for all the simulations.

### 5.1. Load Flow Results for Topology 1

In Topology 1, with the flat start consideration, all the considered scenarios converged in four iterations. The load flow solution for Topology 1 is summarized in Tables 3–5. Simulation results in Table 3 show an improvement in the voltage profile for the given Scenarios (2) and (3).

**Table 3.** Load Flow Results for Topology 1.

Bus Number	Bus Type	Voltage (p.u) (DER at AC Buses)	Voltage (p.u) (DER at AC Buses)	Voltage (p.u) (DER at AC + DC Buses)
1	AC	1.050∠0.000	1.050∠0.000	1.050∠0.000
2	AC	1.045∠−0.126	1.046∠−0.101	1.045∠−0.120
3	AC	1.018∠−0.829	1.025∠−0.656	1.020∠−0.781
4	AC	0.999∠−1.376	1.010∠−1.083	1.002∠−1.293
5	AC	0.979∠−1.970	0.995∠−1.540	0.983∠−1.849
6	DC	1.050	1.050	1.050
7	DC	1.047	1.048	1.047
8	DC	1.039	1.040	1.039
9	DC	1.025	1.029	1.025
10	DC	1.013	1.018	1.013
11	DC	1.012	1.017	1.012
12	DC	1.009	1.015	1.009
13	DC	1.000	1.009	1.000
14	DC	0.997	1.006	0.997
15	DC	0.994	1.004	0.994
16	DC	0.993	1.004	0.993
17	DC	0.989	1.002	0.989
18	DC	0.988	1.001	0.988
19	AC	1.045∠−0.125	1.046∠−0.102	1.045∠−0.121
20	AC	1.045∠−0.114	1.046∠−0.108	1.045∠−0.127
21	AC	1.045∠−0.109	1.046∠−0.110	1.045∠−0.129
22	AC	1.044∠−0.111	1.046∠−0.112	1.045∠−0.131
23	AC	1.018∠−0.830	1.025∠−0.656	1.020∠−0.782
24	AC	1.018∠−0.833	1.024∠−0.667	1.020∠−0.785
25	AC	1.017∠−0.837	1.024∠−0.671	1.019∠−0.789
26	DC	1.048	1.048	1.048
27	DC	1.046	1.046	1.046
28	DC	1.039	1.039	1.039
29	DC	1.036	1.035	1.035
30	DC	1.034	1.032	1.032
31	DC	1.031	1.029	1.029
32	DC	1.031	1.028	1.028
33	DC	1.030	1.028	1.028

In Tables 4 and 5, it is concluded in Scenarios (2) and (3) that with DER connected on DC network cause a decrease in power injection from AC into DC network, resulting in a decrease in AC/DC

converter and network losses. It is apparent from the results in Table 5 that, if the losses of the converter/inverter, which were used for DER integration are considered, the overall losses in Scenario (3) is effectively reduced.

**Table 4.** Summary of Hybrid AC/DC Distribution System Topology 1.

	Topology 1 (DER at AC)	Topology 1 (DER at DC)	Topology 1 (DER at AC + DC)
Power absorbed at DC Slack bus (p.u)	−0.80585	−0.63521	−0.75868
Converter Bus Power (p.u)	−0.8260 + j0.1154	−0.6524 + j0.0357	−0.7780 + j0.0911
AC Grid Power Injection (p.u)	−0.8272 + j0.005	−0.6531 + j0.005	−0.7790 + j0.005
Converter Bus Voltage (p.u)	0.992∠−0.27	0.997∠−0.20	0.993∠−0.25

Figure 5 shows the results of a case study by considering Scenario (3) as a base case. Considering an increase in generation of DER connected on a DC network results a decrease in overall network losses, while assuming DER at AC network, AC and DC network loads to be constant.

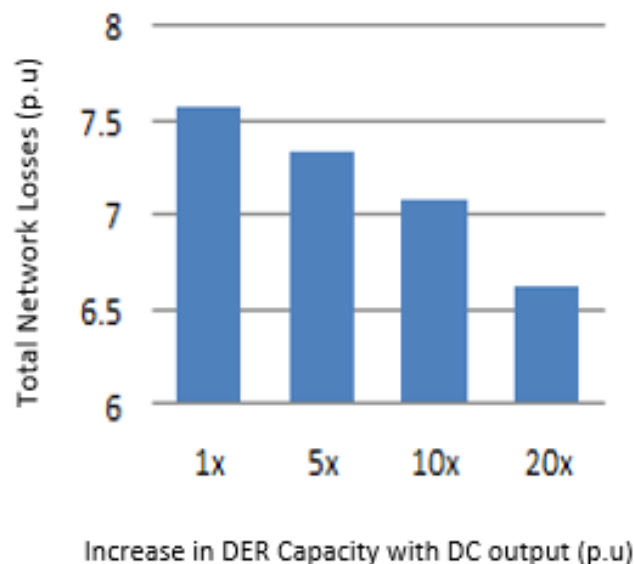


**Figure 5.** Change in Network Losses with increase in DER capacity (DC output).

**Table 5.** Losses in Hybrid AC/DC Distribution System Topology 1.

	Losses (p.u) (DER at AC)	Losses (p.u) (DER at DC)	Losses (p.u) (DER at AC + DC)
AC Line Losses	0.05985 + j0.0305	0.04653 + j0.0186	0.05269 + j0.0268
DC Line Losses	0.0223	0.0173	0.0230
AC/DC Converter Losses	0.0202	0.0172	0.0193
DER Converter Losses	0.0228	0.0229	0.00
Total Losses (without DER Converter)	0.1023 + j0.0305	0.08103 + j0.0186	0.09601 + j0.0268
Total Losses (with DER Converter)	0.1251 + j0.0305	0.10393 + j0.0186	0.09601 + j0.0268

## 5.2. Load Flow Results for Topology 2

In Topology 2, the system with all the proposed scenarios converged in two iterations with the flat start consideration. Tables 6–8 summarize the load flow results for Topology 2. It is observed from

the load flow results that an improvement in the voltage profile occurs for all the given scenarios along with an improved % voltage drop for the proposed Topology 2 as shown in Table 6. In Scenarios (2) and (3), a decrease in power flow from the AC network to DC network along with the minimization in the overall DC line losses as compared to AC line losses was observed, as shown in Table 7.

**Table 6.** Load Flow Results for Topology 2.

Bus Number	Bus Type	Voltage (p.u) (DER at AC Buses)	Voltage (p.u) (DER at AC Buses)	Voltage (p.u) (DER at AC + DC Buses)
1	DC	1.050	1.050	1.050
2	DC	1.049	1.049	1.049
3	DC	1.046	1.047	1.046
4	DC	1.046	1.047	1.046
5	DC	1.046	1.048	1.046
6	AC	1.050∠0.000	1.050∠0.000	1.050∠0.000
7	AC	1.050∠−0.015	1.050∠−0.019	1.050∠−0.013
8	AC	1.050∠−0.022	1.049∠−0.016	1.050∠−0.019
9	AC	1.050∠−0.039	1.049∠−0.022	1.050∠−0.037
10	AC	1.049∠−0.056	1.048∠−0.027	1.049∠−0.053
11	AC	1.049∠−0.058	1.048∠−0.026	1.049∠−0.055
12	AC	1.049∠−0.062	1.048∠−0.025	1.049∠−0.060
13	AC	1.049∠−0.085	1.047∠−0.032	1.049∠−0.082
14	AC	1.049∠−0.095	1.047∠−0.038	1.049∠−0.092
15	AC	1.049∠−0.103	1.047∠−0.041	1.049∠−0.101
16	AC	1.050∠−0.113	1.047∠−0.043	1.050∠−0.111
17	AC	1.050∠−0.128	1.047∠−0.049	1.050∠−0.126
18	AC	1.050∠−0.129	1.047∠−0.050	1.050∠−0.127
19	DC	1.048	1.048	1.048
20	DC	1.043	1.042	1.042
21	DC	1.043	1.041	1.041
22	DC	1.041	1.040	1.040
23	DC	1.045	1.045	1.045
24	DC	1.044	1.044	1.044
25	DC	1.043	1.043	1.043
26	AC	1.050∠−0.003	1.050∠0.003	1.050∠0.003
27	AC	1.050∠−0.006	1.050∠0.008	1.050∠0.008
28	AC	1.050∠−0.024	1.049∠0.014	1.049∠0.014
29	AC	1.049∠−0.037	1.048∠0.021	1.048∠0.021
30	AC	1.049∠−0.043	1.048∠0.029	1.048∠0.029
31	AC	1.050∠−0.072	1.047∠0.022	1.047∠0.022
32	AC	1.050∠−0.080	1.047∠0.020	1.047∠0.020
33	AC	1.050∠−0.081	1.047∠0.020	1.047∠0.020

For the given topology, the results in Table 8 show that, by considering converter/inverter losses used for DER integration, the overall losses in Scenario (3) is minimized as compared to Scenarios (1) and (2). Results have also been compared by not considering the losses of converter/inverter used for DER integration.

**Table 7.** Summary of Hybrid AC/DC Distribution System Topology 2.

	Topology 2 (DER at AC)	Topology 2 (DER at DC)	Topology 2 (DER at AC + DC)
Power absorbed at DC Slack bus (p.u)	−0.41764	−0.32188	−0.36998
Converter Bus Power (p.u)	−0.4317 − j0.0454	−0.3351 − j0.0638	−0.3836 − j0.0552
AC Grid Power Injection (p.u)	−0.4320 + j0.005	−0.3353 + j0.005	−0.3838 + j0.005
Converter Bus Voltage (p.u)	1.042∠−0.10	1.039∠−0.08	1.040∠−0.09

A case study was also done for the given topology by considering an increase in generation of DER capacity connected in an AC network while considering DER at DC network, and AC and DC network loads remain constant in Scenario (3). The results in Figure 6 shows that an increase in network losses occurs with an increase in AC generation.

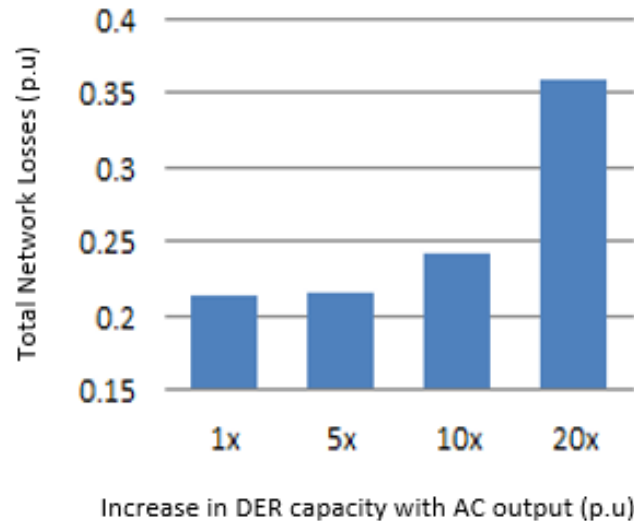


**Figure 6.** Change in Network Losses with increase in DER capacity (AC output).

**Table 8.** Losses in Hybrid AC/DC Distribution System Topology 2.

	Losses (p.u) (DER at AC)	Losses (p.u) (DER at DC)	Losses (p.u) (DER at AC + DC)
AC Line Losses	0.002 + j0.0	0.004 + j0.0	0.003 + j0.0
DC Line Losses	0.019	0.019	0.021
AC/DC Converter losses	0.0141	0.0132	0.0136
DER Converter Losses	0.0229	0.0228	0.00
Total Losses (without DER Converter)	0.0351 + j0.0	0.0362 + j0.0	0.0376 + j0.0
Total Losses (with DER Converter)	0.058 + j0.0	0.059 + j0.0	0.0376 + j0.0

From the comparison of the results in Tables 5 and 8 for both the topologies, it can be concluded that Scenario (3) results a reduction in overall system losses as compared to Scenarios (1) and (2) because of less number of conversion stages. Figure 7 and Table 9 present the comparison of Scenario (3) for both topologies with respect to some other additional factors for the load flow analysis of the AC/DC hybrid distribution networks. It can also be concluded that appropriate placement of DER while considering the network type and DER output also results in a reduction in network power transfer and loss reduction for AC/DC hybrid distribution system. It is also observed that converter losses in VSC-MTDC based network cannot be neglected and plays a significant role in the implementation and planning of AC/DC hybrid distribution network.

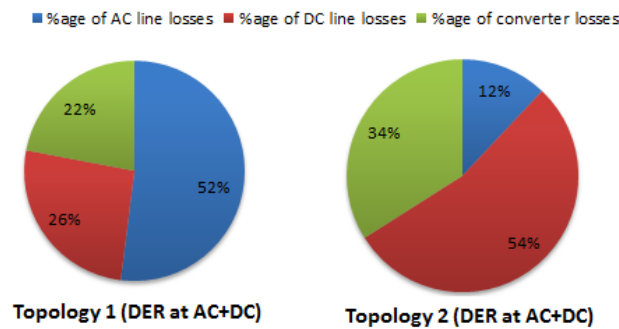


Figure 7. Losses comparison in Scenario (3) for Topologies 1 and 2.

Table 9. Comparison of results for Scenario (3) for Topologies 1 and 2.

	Topology 1 (DER at AC+DC)	Topology 2 (DER at AC + DC)
Max % voltage drop in AC lines	6.38	0.285
Max % voltage drop in DC lines	5.90	0.95
Max Single AC line losses	0.0197 + j0.01 at Line 2–3	0.001 + j0.0 at Line 27–28
Max Single DC line losses	0.0055 at Line 8–9	0.008 at Line 4–5

## 6. Conclusions

This paper has presented the formulation and implementation of a Newton–Raphson (N-R) algorithm for the load flow calculations in AC/DC hybrid distribution network including VSC modeling with the losses and different control modes. The impact of converter and network losses was considered by deployment of two example systems constructed by modifying the IEEE 33 bus hybrid AC/DC distribution network interconnected with MTDC networks. Obtained results show that the appropriate placement of DER in the network while considering the output type is important for the reduction of losses in the network. In addition, the load flow solution depends upon the modeling of the converter and network losses along with the quantity of the converters in the network. The main conclusion that can be drawn from this paper is that proper modeling of converter losses is important, as neglecting the converter losses is not possible in the AC/MTDC network, else it could lead to different load flow values and an incomplete overall network loss assessment. In operational point of view, the converter losses and the number of AC or DC network branches are the issues which should be taken resolved for future planning and expansion of MTDC network.

**Acknowledgments:** This work was supported by Human Resources Program in Energy Technology of the Korea Institute of Energy Technology Evaluation and Planning (KETEP), granted financial resource from the Ministry of Trade, Industry & Energy, Republic of Korea (No. 20164030200980).

**Author Contributions:** Muhammad Omer Khan proposed the original idea and carried out the main research tasks. Saeed Zaman Jamali, Chul-Ho Noh and Gi-Hyeon Gwon contributed to analyzing, writing and summarizing the proposed ideas. Saeed Zaman Jamali and Chul-Hwan Kim double-checked the results and the whole manuscript.

**Conflicts of Interest:** The authors declare no conflict of interest.

## References

1. Asmus, P. Microgrid, virtual power plants and our distributed energy future. *Electr. J.* **2010**, *23*, 72–82.
2. Ritwik, M. Aggregation of microgrids with DC system. *Electr. Power Syst. Res.* **2014**, *108*, 134–143.
3. Blaabjerg, F.; Zhe, C.; Kjaer, S.B. Power electronics as efficient interface in dispersed power generation systems. *IEEE Trans. Power Electron.* **2004**, *19*, 1184–1194.

4. Katiraei, F.; Iravani, R.; Hatziargyriou, N.; Dimeas, A. Microgrids management. *IEEE Power Energy Mag.* **2008**, *6*, 54–65.
5. Hatziargyriou, N.; Asano, H.; Iravani, R.; Marnay, C. Microgrids. *IEEE Power Energy Mag.* **2007**, *5*, 78–94.
6. Xu, L.; Chen, D. Control and operation of a DC microgrid with variable generation and energy storage. *IEEE Trans. Power Deliv.* **2011**, *26*, 2513–2522.
7. Wang, P.; Goel, L.; Liu, X.; Choo, F.H. Harmonizing AC and DC: A hybrid AC/DC future grid solution. *IEEE Power Energy Mag.* **2013**, *11*, 76–83.
8. Kurohane, K.; Senjyu, T.; Yona, A.; Urasaki, N.; Goya, T.; Funabashi, T. A hybrid smart AC/DC power system. *IEEE Trans Smart Grid* **2010**, *1*, 199–204.
9. Liu, X.; Wang, P.; Loh, P.C. A hybrid AC/DC micro-grid. In Proceedings of the 2010 International Power Electronics Conference (IPEC), Singapore, 27–29 October 2010; pp. 746–751.
10. Kwasinski, A. Quantitative evaluation of DC microgrids availability: Effects of system architecture and converter topology design choices. *IEEE Trans. Power Electron.* **2011**, *26*, 835–851.
11. Ding, G.; Gao, F.; Zhang, S. Control of hybrid AC/DC microgrid under islanding operational conditions. *J. Mod. Power Syst. Clean Energy* **2014**, *2*, 223, doi:10.1007/s40565-014-0065-z.
12. Kakigano, H.; Miura, Y.; Ise, T.; Uchida, R.D.C. Micro-grid for super high quality distribution—System configuration and control of distributed generations and energy storage devices. In Proceedings of the IEEE Power Electronics Specialists Conference, Jeju, Korea, 18–22 June 2006; pp. 1–7.
13. Noroozian, R.; Abedi, M.; Gharehpetian, G.B.; Hosseini, S.H. Combined operation of DC isolated distribution and PV system for supplying unbalanced AC loads. *Renew. Energy* **2009**, *34*, 899–1008.
14. Mohamed, A.; Carlos, F.; Ma, T.; Farhadi, M.; Mohammed, O. Operation and protection of photovoltaic systems in hybrid AC/DC smart grids. In Proceedings of the IECON 2012—38th Annual Conference on IEEE Industrial Electronics Society, Montreal, QC, Canada, 25–28 October 2012; pp. 1104–1109.
15. Red, D.F.P. An Overview of the Desertec Concept. 2010. Available online: <http://www.desertec.org/fileadmin/downloads/> (accessed on 08 September 2017).
16. Airtricity European Offshore Supergrid Proposal. 2010. Available online: <http://www.airtricity.com> (accessed on 08 September 2017).
17. Chaudhuri, N.; Majumder, R.; Chaudhuri, B.; Pan, J. Stability analysis of VSC MTDC grids connected to multimachine AC systems. *IEEE Trans. Power Deliv.* **2011**, *26*, 2774–2784.
18. Chen, H.; Wang, C.; Zhang, F.; Pan, W. Control strategy research of VSC based multiterminal HVDC system. In Proceedings of the 2006 IEEE PES Power Systems Conference and Exposition (PSCE'06), Atlanta, GA, USA, 29 October–1 November 2006; pp. 1986–1990.
19. Lago, J.; Heldwein, M.L. Operation and control-oriented modeling of a power converter for current balancing and stability improvement of DC active distribution networks. *IEEE Trans. Power Electron.* **2011**, *26*, 877–885.
20. Guerrero, J.M.; Vasquez, J.C.; Matas, J.; Garcia de Vicuna, L.; Castilla, M. Hierarchical control of droop-controlled AC and DC microgrids—A general approach toward standardization. *IEEE Trans. Ind. Electron.* **2011**, *58*, 158–172.
21. Tang, L.; Ooi, B. Locating and isolating DC faults in multi-terminal DC systems. *IEEE Trans. Power Deliv.* **2007**, *22*, 1877–1884.
22. Tang, L.; Ooi, B.T. Protection of VSC-multi-terminal HVDC against DC faults. In Proceedings of the IEEE 33rd Annual Power Electronics Specialists Conference (PESC 02), Cairns, Australia, 23–27 June 2002; pp. 719–724.
23. Chen, X.; Sun, H.S.; Wen, J.Y.; Lee, W.J.; Yuan, X.F.; Li, N.; Yao, L.Z. Integrating wind farm to the grid using hybrid multiterminal HVDC technology. *IEEE Trans. Ind. Appl.* **2011**, *47*, 965–972.
24. Cole, S.; Beerten, J.; Belmans, R. Generalized dynamic VSC MTDC model for power system stability studies. *IEEE Trans. Power Syst.* **2010**, *25*, 1655–1662.
25. Beerten, J.; Cole, S.; Belmans, R. Generalized steady-state VSC MTDC model for sequential AC/DC power flow algorithms. *IEEE Trans. Power Syst.* **2012**, *27*, 821–829.
26. Baradar, M.; Ghandhari, M. A multi-option unified power flow approach for hybrid AC/DC grids incorporating multi-terminal VSC-HVDC. *IEEE Trans. Power Syst.* **2013**, *28*, 2376–2383.
27. Zhang, X.P. Multiterminal voltage-sourced converter-based HVDC models for power flow analysis. *IEEE Trans Power Syst.* **2004**, *19*, 1877–1884.

28. Gengyin, L.; Ming, Z.; Jie, H.; Guangkai, L.; Haifeng, L. Power flow calculation of power systems incorporating VSC-HVDC. In Proceedings of the 2004 International Conference on Power System Technology (Power Con), Singapore, 21–24 November 2004; Volume 2, pp. 1562–1566.
29. Acha, E.; Kazemtabrizi, B.; Castro, L.M. A new VSC HVDC model for power flows using the Newton Raphson method. *IEEE Trans. Power Syst.* **2013**, *28*, 2602–2612.
30. Chen, Q.; Tang, G.-Q.; Xun, W. AC–DC power flow algorithm for multi-terminal VSC-HVDC systems. *Electr. Power Automot. Equip.* **2005**, *25*, 1–6.
31. Wang, W.; Barnes, M. Power flow algorithms for multi-terminal VSC-HVDC with droop control. *IEEE Trans. Power Syst.* **2014**, *29*, 1721–1730.
32. VSC TRANSMISSION. CIGRE Working Group B4.37; Technical Report Ref.269; April 2005. Available online: <http://www.e-cigre.org/> (accessed on 22 September 2017).
33. Zhao, Q.; García-González, J.; Gomis-Bellmunt, O.; Prieto-Araujo, E.; Echavarren, F.M. Impact of converter losses on the optimal power flow solution of hybrid networks based on VSC-MTDC. *Electr. Power Syst. Res.* **2017**, *151*, 395–403.
34. Liang, H.; Zhao, X.; Yu, X.; Gao, Y.; Yang, J. Study of power flow algorithm of AC/DC distribution system including VSC-MTDC. *Energies* **2015**, *8*, 8391–8405.
35. Cao, J.; Du, W.; Wang, H.; Bu, S. Minimization of transmission loss in meshed AC/DC grids with VSC-MTDC networks. *IEEE Trans. Power Syst.* **2013**, *28*, 3047–3055.
36. Nilsson, D.; Sannino, A. Efficiency analysis of low- and medium- voltage DC distribution systems. In Proceedings of the IEEE Power Engineering Society General Meeting, Denver, CO, USA, 6–10 June 2004; pp. 2315–2321.
37. Hammerstrom, D.J. AC versus dc distribution systems—Did we get it right? In Proceedings of the Power Engineering Society General Meeting, Tampa, FL, USA, 24–28 June 2007; pp. 1–5.
38. Teng, J.H. Modelling distributed generations in three-phase distribution load flow. *IET Gener. Transm. Distrib.* **2008**, *2*, 330–340.
39. Mousavizadeh, M.S.; Shariatkhah, M.H.; Haghifam, M.R. Load Flow Analysis for AC/DC Distribution Systems with Distributed Generations. *Electr. Power Compon. Syst.* **2017**, *45*, 1057–1067, doi:10.1080/15325008.2017.1318321.
40. MATPOWER Website. Available online: <http://www.pserc.cornell.edu/matpower/> (accessed on 22 November 2016).
41. Siemens. HVDC PLUS-Basics and Principle of Operation. 2008. Available online: <http://www.siemens.com/energy/hvdcplus> (accessed on 14 March 2017).
42. Bose, B.K. *Power Electronics and Motor Drives: Advances and Trends*; Academic Press: Cambridge, MA, USA, 2010.
43. Oates, C.; Davidson, C. A comparison of two methods of estimating losses in the Modular Multi-Level Converter. In Proceedings of the 2011 14th European Conference on Power Electronics and Applications (EPE 2011), Birmingham, UK, 30 August–1 September 2011; pp. 1–10.
44. Haugland, P. *It's Time to Connect—Technical Description of HVDC Light Technology*; ABB, Technical Report; ABB Power Technologies; 2008. Available online: <http://new.abb.com/systems/hvdc/hvdc-light> (accessed on 20 November 2017).
45. *Guide for the Development of Models for HVDC Converters in a HVDC Grid*; CIGRE Working Group B4.57; 2014. Available online: <http://www.e-cigre.org/> (accessed on 10 November 2017).
46. Daelemans, G. VSC HVDC in Meshed Networks. Master's Thesis, Katholieke Universiteit Leuven, Leuven, Belgium, 2008.
47. Beerten, J.; Van Hertem, D.; Belmans, R. VSC MTDC systems with a distributed DC voltage control—A power flow approach. In Proceedings of the 2011 IEEE Trondheim PowerTech, Trondheim, Norway, 19–23 June 2011.
48. Rich Christie, "Power Systems Test Case Archive". Available online: <http://www.ee.washington.edu/research/pstca> (accessed on 4 February 2016).

